

Supplementary Information for

Enhanced Responsivity of Graphene/Si-based Heterostructure

Broadband Photodetector by Introducing a WS₂ Interfacial Layer

Tianying He[†], Changyong Lan[†], Sihan Zhou[†], Yongjun Li[†], Yi Yin[†], Chun Li^{†,‡,*}, Yong Liu

[†]State Key Laboratory of Electronic Thin Films and Integrated Devices, and School of Optoelectronic Science and Engineering, University of Electronic Science and Technology of China

[‡]Huazhong University of Science and Technology Wuhan National Laboratory for Optoelectronics

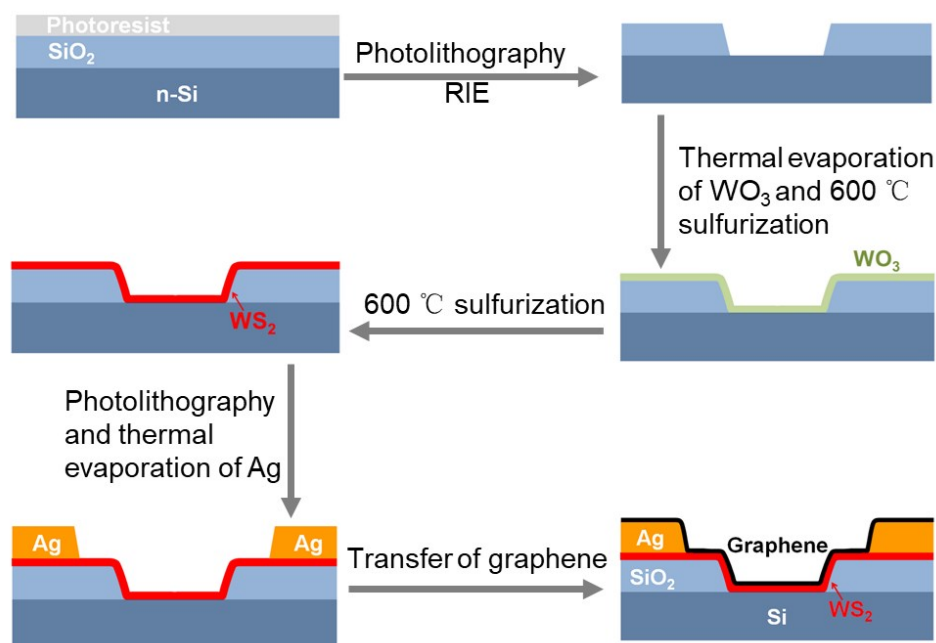


Figure S1. Schematic of device fabrication process. An n-type Si with 285 nm thermally oxidized SiO₂ was selected as the substrate, which was cleaned with acetone, alcohol, and deionized water for 5 min each under ultrasonication sequentially and blow-dry with N₂. The substrate was first patterned by standard UV-lithography technique and then etched by reactive ion etching method, forming circular holes with radius of 5 μm. Next, WO₃ film was deposited on the substrate by thermal evaporation method, which was sulfurized into WS₂ in a high temperature (600°C) tube furnace using sulfur powder as sulfur source at a low pressure (120 Pa). After that, ring shaped Ag electrode (inner diameter: 10 μm, outer diameter: 210 μm) was deposited by combining photolithography and thermal evaporation techniques. The electrode enclosed area contains both the WS₂/SiO₂/Si region and WS₂/Si junction region. The large width (200 μm) of the electrode can prevent photocurrent contribution from the outside area of the electrode. Finally, monolayer graphene was transferred on the WS₂ film, forming graphene/WS₂/Si heterostructure.

* Author to whom any correspondence should be addressed. E-mail: lichun@uestc.edu.cn

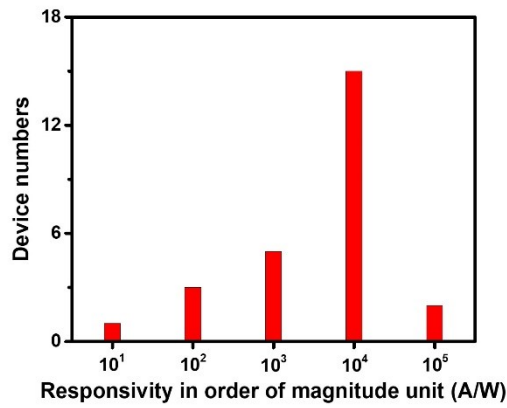


Figure S2. Statistics of photoresponsivities in order of magnitude unit of 26 as-fabricated photodetectors (Gr/10.9 nm WS₂/Si devices) under illumination (650 nm) with light intensity of 19 $\mu\text{W}/\text{cm}^2$ at -5 V.

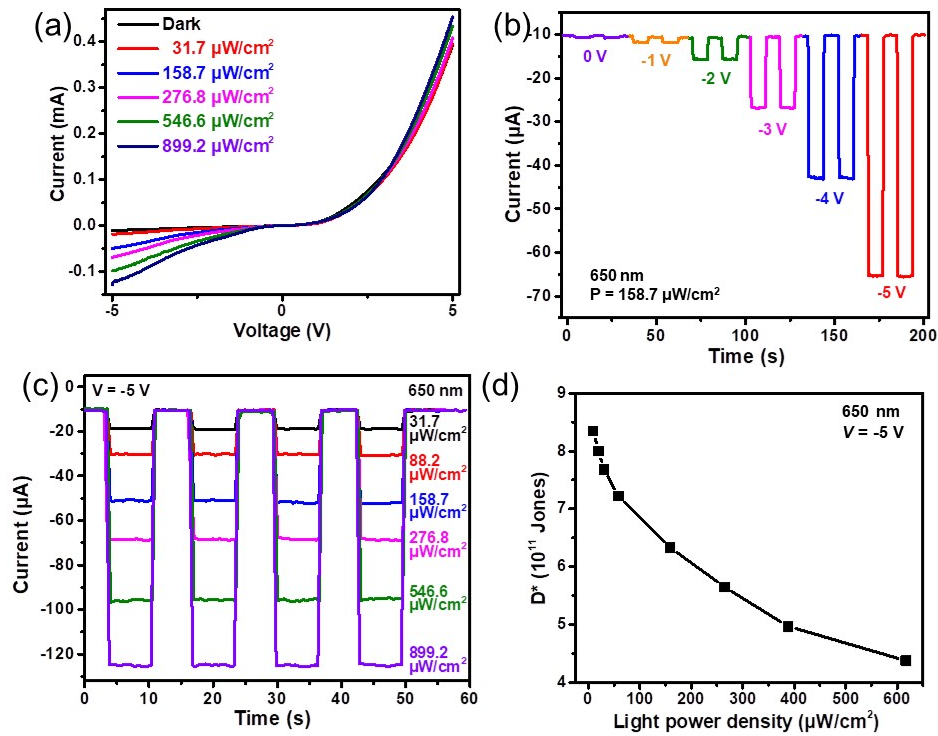


Figure S3. Optoelectronic properties of the device Gr/10.9 nm WS₂/Si. (a) I - V curves of the device without and with light illumination (650 nm). (b) Photocurrent as a function of time under different bias voltage. (c) Temporal response of the device measured under modulated light illumination (650 nm) with varied light intensity at -5 V. The photocurrent approaches about 0.12 mA when the light intensity is about 889.2 $\mu\text{W}/\text{cm}^2$. (d) Specific detectivity (D^*) as a function of light intensity. The device exhibits a high D^* of 8.35×10^{11} Jones under 8.8 $\mu\text{W}/\text{cm}^2$.

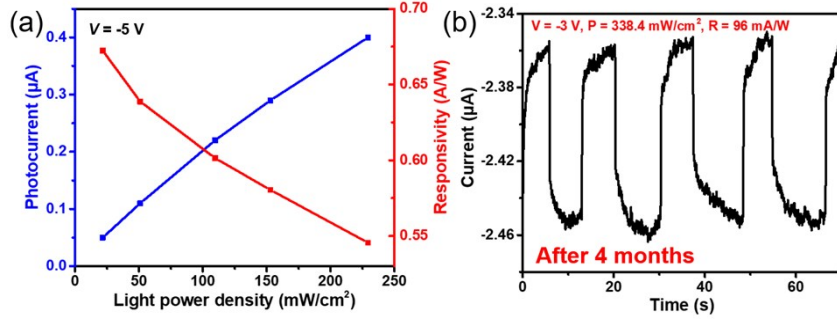


Figure S4. Photoresponse properties of the device Gr/10.9 nm WS₂/Si at 1550 nm. (a) Photocurrent and corresponding responsivity (R) as a function of light intensity. The device shows a high R of 740 mA/W under 21.7 mW/cm². (b) Temporal response of the device measured under 338.4 mW/cm² after 4 months at -3 V. The device exhibits significant photoresponse even if stored in a low vacuum sample storage cabinet for 4 months, and shows an R of 96 mA/W.

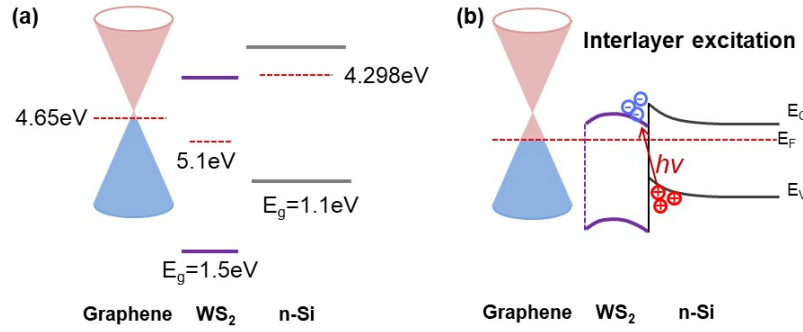


Figure S5. (a) Schematic of band alignment of the graphene, WS₂ and n-Si before contact. (b) The interlayer excitation of the WS₂/Si heterojunction under light illumination. The work function of graphene is slightly larger than the intrinsic value (~ 4.56 eV) due to low level of p-type doping owing to the substrate, metal doping, water molecules in the air.^[1] The work function of undoped WS₂ changes from 4.9 to 5.1 eV corresponding to monolayer and bulk materials, respectively.^[2-4] The phosphorus doping concentration of n-Si is $N_D = 2 \times 10^{15}$ cm⁻³. And the intrinsic carrier concentration of silicon is $N_C = 2.8 \times 10^{19}$ cm⁻³. We can calculate the Fermi Level of this n-Si by the semiconductor doped theory:^[5]

$$E_n = E_C - E_F = -k_0 T \ln(N_D/N_C)$$

$$E_F = \varphi + E_n$$

Where E_C is the conduction band level, E_F is the Fermi level, k_0 is the Boltzmann constant, T is the absolute temperature, φ is the electron affinity. Thus, the Fermi level of the n-Si 4.298 eV is obtained.

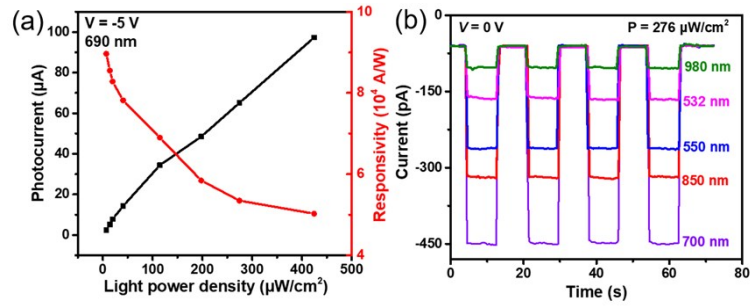


Figure S6. Photoresponse characteristics of the device Gr/10.9 nm WS₂/Si. (a) Photocurrent and responsivity as a function of light intensity. The device presents an ultrahigh R of 8.96×10^4 A/W under 6.9 $\mu\text{W}/\text{cm}^2$. (b) Temporal response of the device measured under 276 $\mu\text{W}/\text{cm}^2$ at zero bias voltage.

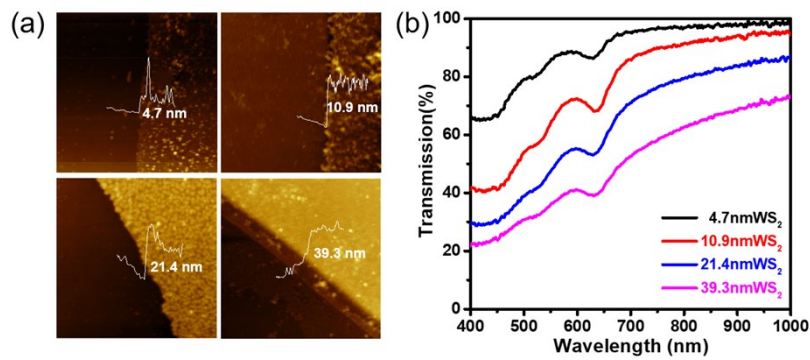


Figure S7. Comparison of different WS₂ films. (a) Atomic force microscope images and (b) transmittance of the different-thickness WS₂ films on quartz substrate.

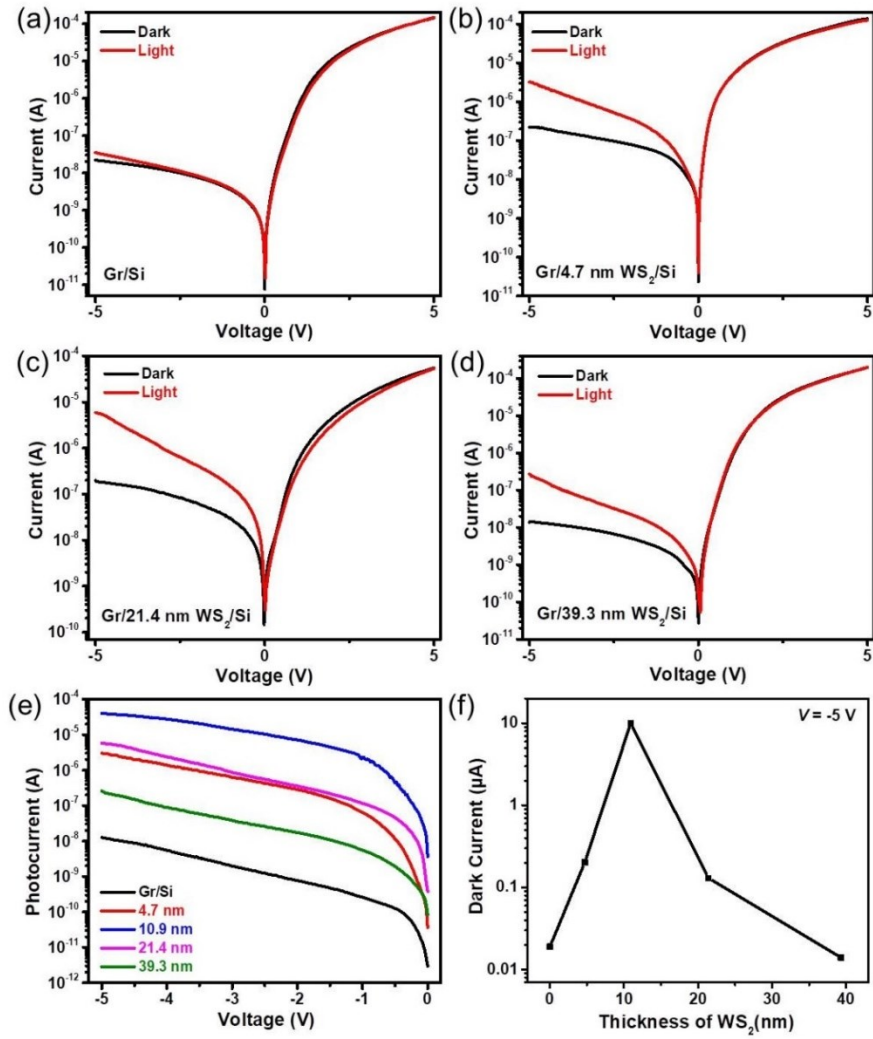


Figure S8. Optoelectronic properties of the Gr/WS₂/Si devices with varied thickness of WS₂ film. *I-V* curves of the Gr/Si (a) and Gr/WS₂/Si devices with WS₂ thickness of 4.7 nm (b), 21.4 nm (c), and 39.3 nm (d) under dark and 650 nm light illumination of 276.8 μW/cm². (e) Photocurrent of the Gr/WS₂/Si devices with varied thickness of WS₂ film along with the change of voltage extracted from (a) to (d). (f) Dark current of the Gr/WS₂/Si devices as a function of WS₂ thickness under -5 V.

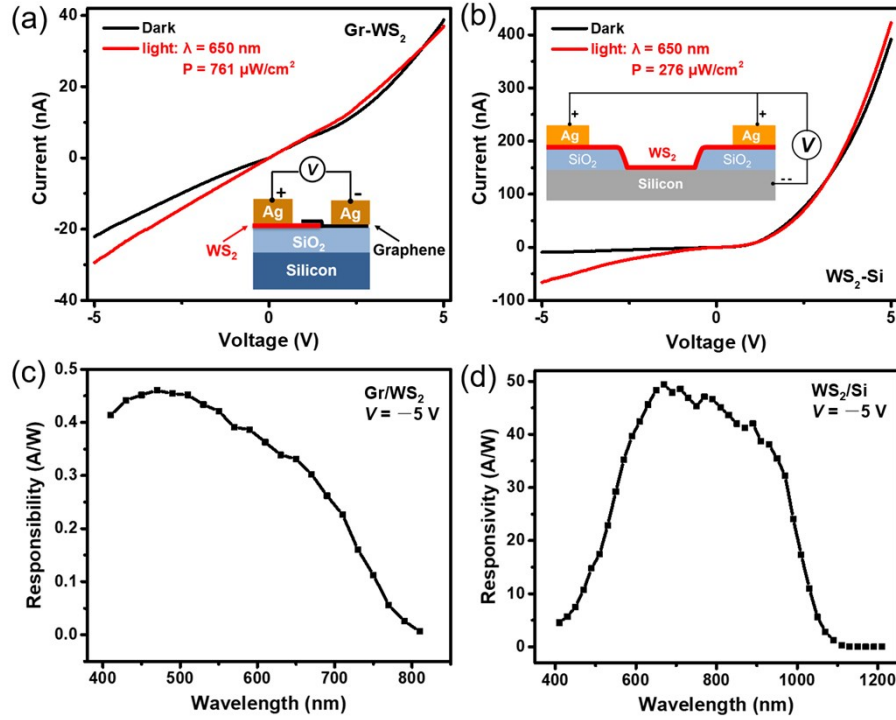


Figure S9. Optoelectronic properties of Gr/WS₂ and WS₂/Si devices. (a) I - V curves of the Gr/WS₂ device under dark and light illumination of 761 $\mu\text{W}/\text{cm}^2$. (b) I - V curves of the WS₂/Si device under dark and light illumination of 276 $\mu\text{W}/\text{cm}^2$. (c) Spectral response of the Gr/WS₂ device in the wavelength range of 400-810 nm under constant light intensity of 54 $\mu\text{W}/\text{cm}^2$ at reverse bias -5 V. (d) Spectral response of the WS₂/Si device in the wavelength range of 400-1200 nm under constant light intensity of 33 $\mu\text{W}/\text{cm}^2$ at reverse bias -5 V. The Gr/WS₂ device presents a lower photocurrent (7.4 nA under light intensity of 761 $\mu\text{W}/\text{cm}^2$ at -5 V) than that in the WS₂/Si device (56.7 nA under light intensity of 276 $\mu\text{W}/\text{cm}^2$ at -5 V), indicating that the WS₂/Si heterostructure exhibits higher photosensitivity than Gr/WS₂ heterojunction. The Gr/WS₂ device shows a cutoff wavelength of 810 nm. The responsivity of WS₂/Si device drops sharply around 1100 nm corresponding to the cutoff wavelength of the absorption spectrum in intrinsic Si, indicating that light response mainly occurs in Si. Moreover, for the Gr/Si, Gr/WS₂, WS₂/Si photodetectors, the responsivities are in the range of hundreds of mA/W to dozens of A/W, much lower than that in Gr/WS₂/Si photodetectors, which clarifies that the introduction of WS₂ interfacial layer plays a vital role in improving the performance of Gr/Si-based devices.

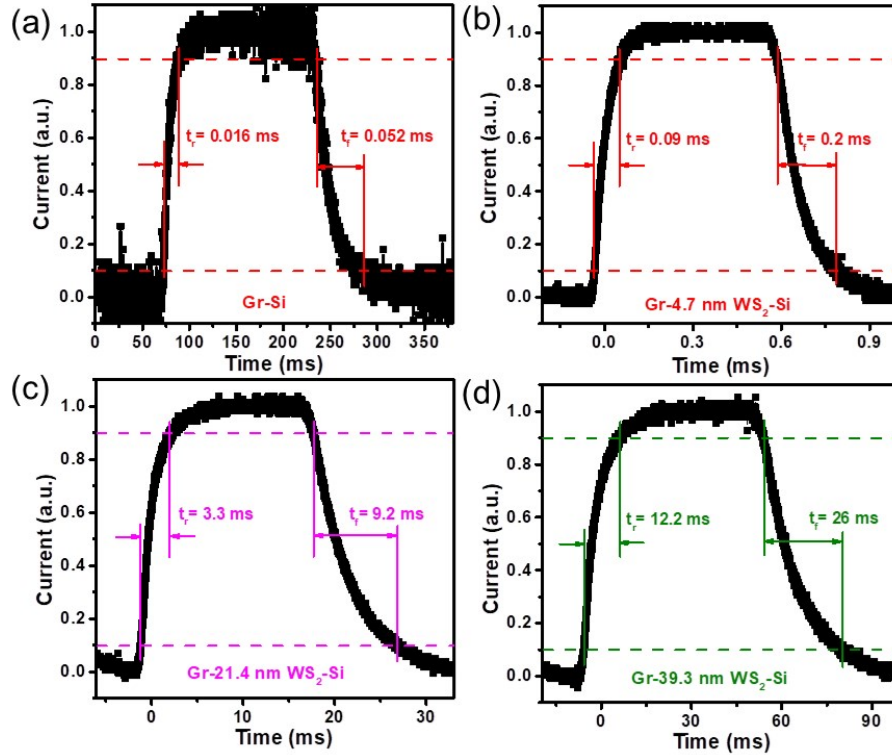


Figure S10. High resolution time-resolved curves of the Gr/WS₂/Si devices with different thickness of WS₂ film.

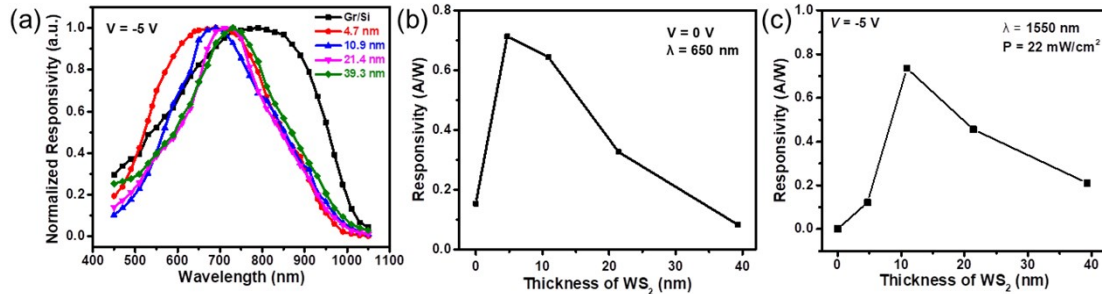


Figure S11. Spectral response characteristics of the Gr/WS₂/Si devices with different thickness of WS₂ film. (a) The normalized responsivity as a function of wavelength (450-1050 nm). (b, c) The responsivity of the Gr/Si and Gr/WS₂/Si devices as a function of WS₂ thickness under 650 nm light illumination at 0 V (b) and 1550 nm light illumination at -5 V (c).

Reference:

1. Tuning the Graphene Work Function by Electric Field Effect. *Nano Lett.* **2009**, *90*, 3430-3434.
2. Yun, W. S.; Han, S. W.; Hong, S. C.; Kim, I. G.; Lee, J. D. Thickness and Strain Effects on Electronic Structures of Transition Metal Dichalcogenides: 2H-MX₂ Semiconductors (M=Mo, W; X=S, Se, Te). *Phys. Rev. B* **2012**, *85*, 033305.

3. Yu, Y.; Fong, P. W. K.; Wang, S.; Surya, C. Fabrication of WS₂/GaN p-n Junction by Wafer-Scale WS₂ Thin Film Transfer. *Sci. Rep.* **2016**, *6*, 37833.
4. Kong, D.; Wang, H.; Cha, J. J.; Pasta, M.; Koski, K. J.; Yao, J.; Cui, Y. Synthesis of MoS₂ and MoSe₂ Films with Vertically Aligned Layers. *Nano Lett.* **2013**, *13*, 1341-1347.
5. Sze, S. M.; Ng, K. K. *Physics of Semiconductor Devices*. John Wiley & Sons **2006**.